Long-Term Energy Transition Scenarios in Weakly Interconnected Countries: Implications for Frequency Stability and Reserve Requirements

Marco Navia[1*], Sergio Balderrama[2], Matija Pavicevic[3], Sylvain Quoilin[1]

[1]Université de Liège, Quartier Polytech 1, Allée de la Découverte, 17, Sart Tilman, Liège, 4000, Liège, Belgium

[2]Universidad Mayor de San Simon, Calle Sucre y parque la Torre, Cochabamba, Cochabamba, Bolivia

[3]UC Louvain la Neuve, Place du Levant 2/L5.04.03, 1348 Louvain-la-Neuve, Louvain, 3000, Louvain, Belgium

Corresponding Author: manavia@uliege.be

ABSTRACT

The global energy transition, driven by the Sustainable Development Goals and commitments to decarbonization, is transforming power systems with a rapid shift towards renewable energy sources. While this transition offers environmental and economic benefits, it poses significant operational challenges, particularly in maintaining frequency stability and ensuring adequate reserves. This study addresses these challenges, focusing on countries with vast renewable energy potential but isolated or weakly interconnected power systems prone to frequency instability. Presenting Bolivia as a notable case study in the global south, this research harmonizes and adapts long-term energy planning scenarios for 2050, derived from energy planning framework developed with Energy System Optimization Models, as inputs to an energy model aimed at Unit Commitment and Optimal Dispatch. This work integrates a multisectoral long-term planning perspective with detailed temporal and spatial resolution analysis that includes operational constraints to evaluate system stability and reserve requirements. The methodology involves an exogenous stability analysis to quantify system inertia response, fast frequency reserve, and primary frequency reserve needs, based on the (n-1) contingency criterion. For Bolivia, the dispatch results shows the largest contingency at 400 MW. In the long-term planning scenarios projected for 2050, the total amount of system inertia available relative to the overall size of the power system is expected to be significantly lower than in 2022, reflecting the decommissioning of fossil fuel power plants and the increasing penetration of renewable energy sources. This decline necessitates different balancing services to maintain frequency stability. The study highlights that appropriate reserve sizing is crucial for maintaining stability under low-inertia conditions. In the case study, reserves are adequately sized. Fast frequency reserve requirements range from 60 MW to 454 MW, while the available capacity from BESS averages between 321 MW and 1133 MW. Similarly, primary frequency reserve requirements range from 43 MW to 105 MW, while the available capacity from committed generators providing this service averages between 87 MW and 116 MW. These findings underscore the dependency of reserve availability on the dispatch of flexible generation resources. By bridging long-term energy planning with operational-level analysis, this study offers a replicable framework for evaluating system stability and reserve needs in future power systems, particularly for developing countries navigating the transition to resilient, low-carbon energy systems.

1 INTRODUCTION

The transition toward cleaner energy systems has accelerated the deployment of Variable Renewable Energy (VRE), increasing the variability and uncertainty of net demand. This highlights the need to incorporate short-term operational constraints into long-term planning models (Palmintier & Webster, 2011). Several studies propose frameworks that link long-term planning models with Unit Commitment and Economic Dispatch (UCED) models to better capture system flexibility and operational feasibility (Helgesen & Tomasgard, 2018). As conceptualized by (Helgesen & Tomasgard, 2018), soft-linking Energy System Optimization Models (ESOM) with UCED models can adress this challange. Hamdi et al. (2024) shows that integrating operational aspects into long-term energy planning improves result accuracy and helps manage VRE variability. Additionally, Helistö et al. (2019) highlights that this integration supports the assessment of flexibility needs, such as ramping and reserve requirements, which are essential for maintaining grid stability during the renewable transition. Pavičević et al. (2022) introduces a bi-directional soft-link between EnergyScope and Dispa-SET, capturing short-term variability, sizing flexibility needs, and achieving stable convergence within two iterations. Pavičević (2023) builds on this by applying uni- and bi-directional soft-linking to the electricity and heating sectors, refining ESOM outputs with UCED detail to enhance system adequacy and assess sector coupling for carbon neutrality. Koltsaklis et al. (2017) presents a mixed-integer linear programming (MILP) model integrating UCED with long-term Generation Expansion Planning (GEP), combining operational constraints with strategic investment decisions to support policy and planning. Henke et al. (2024) compares Integrated Assessment Models (IAMs) and ESOMs, emphasizing the value of linking diverse modeling approaches for policy insights and advocating for harmonized structures to enable cross-model scenario comparison. In a two-part study, Jimenez Zabalaga et al. (2024) and Fernandez Vazquez et al. (2024) introduce the "Two-Step Cascade Modeling" framework, which combines EnergyScope for national, long-term transition pathways (Part A) with PyPSA for detailed, spatially resolved power sector modeling (Part B). This approach adds generation, transmission, and storage dynamics within a linkage between two long-term energy models.

While previous studies have improved long-term energy planning by incorporating operational aspects such as capacity expansion, adequacy, system dynamics, and flexibility, none have explicitly integrated frequency stability analysis within a soft-linked framework between UCED and ESOM models. To address this gap, this study proposes a unidirectional soft-linking approach that connects long-term scenarios from ESOMs to a UCED model, using an enhanced version of the frequency stability assessment method originally developed by Navia et al. (2023).

The methodology is applied to Bolivia, using energy transition pathways developed through the Two-Step Cascade Modeling framework (Fernandez Vazquez et al., 2024; Jimenez Zabalaga et al., 2024). Unlike conventional approaches that allow unconstrained VRE expansion, this framework limits renewable deployment based on operational feasibility, helping identify the saturation point of VRE under stability constraints.

The main objective is to bridge high-level energy planning with detailed operational validation, contributing to the development of secure, flexible, and realistic decarbonization pathways—particularly in isolated or weakly interconnected power systems with growing shares of VRE.

The specific contributions of this study include:(i) the harmonization and integration of long-term energy policy scenarios in UCED models, (ii) the dimensioning of the stability requirements necessary to achieve the objectives defined in these scenarios, raised by long-term planning models. These requirements include: System Inertia Response (SIR), Primary Frequency Reserves (PFR) and Fast Frequency Reserves (FFR), (iii) the evaluation of operational limitations in expansion plans under different energy transition scenarios, (iv) the assessment of complementary flexibility and adequacy, of technologies such as transmission lines, or battery energy storage systems (BESS), within the UCED model.

2 METHODS

2.1 Workflow of the Soft-Link Process Between Models

This section describes the workflow of the soft-linking process between the ESOM models (EnergyScope and PyPSA) and the UCED model (Dispa-SET)("The Dispa-SET model — Documentation", n.d.), represented in Figure 1. This integration bridges long-term planning and short-term operational modeling, with a particular focus on frequency stability constraints.

The workflow follows six key stages:

1. **Defining Long-Term Planning Scenarios:** Long-term scenarios for the Bolivian power system are developed based on the methodology proposed by (Jimenez Zabalaga et al., 2024) and (Fernandez Vazquez et al., 2024). These scenarios capture projections of electricity costs, demand, generation mix, capacity expansion, hydrology, VRE potential, and storage. They provide a projected expansion of the power system to ensure generation-demand balance, while also capturing the evolving impact of cross-sectoral interactions on the power system. They are spatially disaggregated and formulated through myopic pathway optimization for selected future years under alternative policy assumptions. These scenarios serve as key inputs for the subsequent UCED analysis.

2. **Data Harmonization and integration into UCED:** Scenario outputs are harmonized and integrated into Dispa-SET, which operates at finer temporal and spatial resolution. Harmonization includes aligning cost and operational constraints and incorporating additional dynamic and technical constraints—e.g., ramping, start-up/shut-down, and minimum stable load—that are typically absent in long-term models. A key enhancement is the introduction of frequency stability constraints in the UCED formulation.

3. **Execution of the UCED model and stability assessment:** Building on the work done by Navia et al. (2023), the swing equation is solved under (n-1) contingency to ensure compliance with stability metrics: Rate of Change of Frequency (RoCoF), frequency nadir, and steady-state deviation. The algorithm computes SIR and PFR requirements externally, which are then enforced in a subsequent UCED simulation. This paper introduces two algorithmic improvements: (i) the incorporation of FFR, and (ii) the replacement of the Incremental Step iteration with Binary Search.

4. **Assessment of modeling accuracy and errors:** Is validated by ensuring that operating conditions are consistently met at each instant and across the simulation horizon. The analysis identifies potential numerical inconsistency such as infeasibility or convergence issues, ensuring reliability and robustness. This specific assessment is not presented in this work due to space limitations.

5. **Comparison and evaluation of results:** UCED outputs are compared against those of the ESOMs to assess consistency in key indicators—adequacy, flexibility, and stability. This step determines whether long-term scenarios remain operationally feasible under high-resolution constraints, particularly when frequency stability is explicitly enforced.

6. **Analysis of Long-Term Planning Assumptions:** Insights from the UCED simulations inform the re-assessment of long-term planning assumptions. Recommendations are derived regarding the inclusion of frequency reserve requirements, adequacy margins, or VRE curtailment needs to enhance the operational feasibility and efficiency of the expansion pathways.

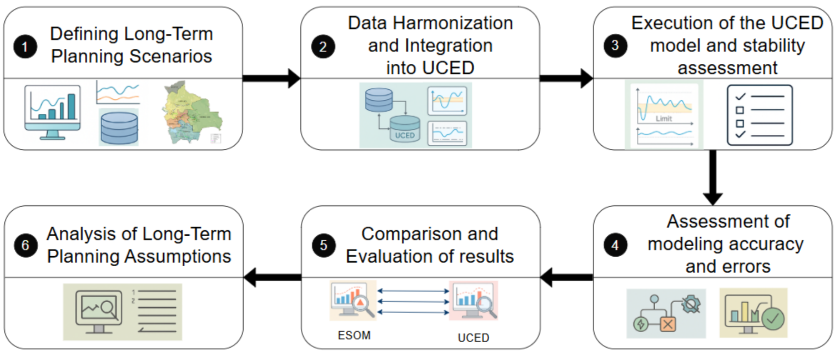

Figure 1: Workflow of the soft-linking between ESOM and UCED models

2.2 Frequency Stability Assessment

The Algorithm for Frequency Stability Assessment (AFSA) presented by Navia et al. (2023) dynamically adjusts SIR and PFR to maintain frequency stability. However, the original version of the AFSA did not consider FFR, which rapidly responds to frequency deviations before PFR take effect. In the present work, the FFR is integrated, allowing a more accurate representation of frequency reserve services in modern power systems[1]. The assessment consists of externally solving the swing equation, which describes the system's dynamic behavior following an imbalance, using data exported from a preliminary UCED simulation. The resulting requirements are then integrated back into the UCED model as additional constraints. The model is subsequently re-run with these new constraints to ensure that the dispatch decisions account for dynamic stability requirements. The algorithm is illustrated in Figure 2.

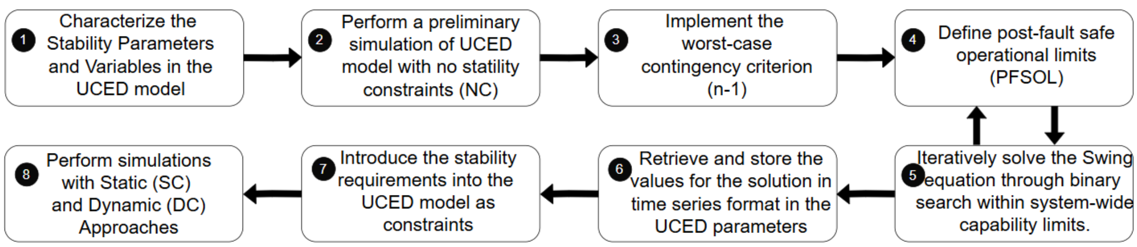

Figure 2: Algorithm for Frequency Stability Assessment

Step 1: Imply the characterization of new input parameters and output variables in the UCED model, essential for implementing the stability constraints and sizing the reserves required to ensure frequency stability.

[1] In the differential equation model of the swing equation, variables and parameters are typically represented using acronyms or single-letter notations (e.g., SIR), whereas in the UCED model formulations, more descriptive names are used (e.g., $SystemInertia$)

Table 1: New parameters and variables characterized in the UCED model

Parameters	$InertiaConstant_u$	$Droop_u$	$MinSystemInertia_i$	$MinFastReserve_i$	$MinPrimaryReserve_i$
Variables	–	–	$AvaSystemInertia_i$	$AvaFastReserve_i$	$AvaPrimaryReserve_i$

Step 2: Consists of running an initial UCED model simulation without frequency stability constraints, referred to as the None-Constraints (NC) approach. This simulation provides the initial dispatch output data including: $Committed_{cu,i}$, $OutputPower_{u,i}$ and $PowerCapacity_{cu,i}$. This data is required for the frequency stability assessment and also serves as a reference to evaluate whether long-term planning scenarios are operationally feasible under frequency stability requirements, as well as to assess their impact on key operational variables of the power system.

Step 3: Implementation of the (n-1) criterion, in which the contingency is defined as the largest generator infeed, and is calculated using two methods. The first presented in Eq 1, computes the contingency over the entire optimization horizon, while the second presented in Eq 2 determines instantaneous contingencies at each time step.

$$CTG = \max_{u,i} \left(OutputPower_{u,i}\right) \tag{1}$$

$$CTG_i = \max_{u} \left(OutputPower_{u,i}\right) \tag{2}$$

Step 4: To ensure frequency stability, the Transmission System Operator (TSO) defines a set of Post-Fault Safe Operational Limits (PFSOL), which specify thresholds for three key indicators: the Rate of Change of Frequency ($MinRoCoF$), the frequency nadir ($Minfnadir$), and the steady-state frequency deviation ($Min\Delta fss$).

Step 5: The system's frequency dynamics following a contingency are governed by the swing equation, shown in Eq. 3.

$$\frac{2 \cdot SIR_i}{f_o} \cdot \frac{d\Delta f_{COI}}{dt} = CTG_i + FFR_i + PFR_i \tag{3}$$

where:

$$FFR_i = k1_i \cdot \Delta f_{COI} \qquad \forall \quad t \geq t_o + t_{Delay} \tag{4}$$

$$PFR_i = k_i \cdot \Delta f_{COI} \qquad \forall \quad t \geq t_o + t_{Preparation} \tag{5}$$

The frequency stability problem can be conceptualized as solving three, nonlinear inequalities derived from system dynamics:

$$RoCoF = \min_t \left(\frac{d\Delta f_{COI}}{dt}\right) \geq MinRoCoF \tag{6}$$

$$fnadir = f_o - \min_t \left(\Delta f_{COI}\right) \geq Minfnadir \tag{7}$$

$$\Delta fss = \Delta f_{COI}(t = 60) \geq Min\Delta fss \tag{8}$$

And these at the same time are implicitly function of contingency (CTG) and the contributions from system inertial response (SIR), fast frequency reserve (FFR), and primary frequency reserve (PFR). The objective is to determine, through a binary search for each CTG_i, the minimum combination of SIR_i, FFR_i, and FFR_i that satisfies the frequency stability constraints (PFSOL criteria) presented in Eq 6 to Eq 8. The search range is performed within system-wide capabilities to provide these frequency services. This approach significantly reduces computational burden by efficiently narrowing the search space for each parameter.

Step 6: The combination of minimum values that solves the swing equation meeting the PFSOL is stored in their respective associated parameter of the UCED model in time series format with its respective index.

Step 7: The UCED model aims to optimize the short-term operation of power systems by minimizing total costs. The details of the original formulation can be found in the model documentation. The stability requirements are introduced as the following new constraints into the UCED model:

$$MinSystemInertia_i \leq AvaSystemInertia_i = \frac{\sum_{cu} PowerCapacity_{cu} \cdot Committed_{cu,i} \cdot InertiaConstant_{cu}}{ConversionFactor} \tag{9}$$

$$MinFastReserve_i \leq AvaFastReserve_i \leq \sum_{ba} \frac{PowerCapacity_{ba} \cdot Committed_{ba,i}}{Droop_{ba} \cdot SystemFrequency} \cdot DeltaFrequencyMax \tag{10}$$

$$MinPrimaryReserve_i \leq AvaPrimaryReserve_i \leq \sum_{cu} \frac{PowerCapacity_{cu} \cdot Committed_{cu,i}}{Droop_{cu} \cdot SystemFrequency} \cdot DeltaFrequencyMax \tag{11}$$

Step 8: To evaluate the impact of introducing different stability requirements, three approaches of UCED simulations are performed as follows:

- NC (Approach with None Constraints): Simulations performed without stability requirements.
- SC (Approach with Static Constraints): Simulations incorporating static constraints for stability.
- DC (Approach with Dynamic Constraints): Simulations applying dynamic constraints for stability.

3 CASE STUDY AND SCENARIOS

Bolivia's power system is among the most isolated in Latin America. Although future cross-border interconnections with neighboring countries are under evaluation, they are not considered in this study. The model preserves the current zonal topology of the system, divided into four areas: Central (CE), Eastern (OR), Northern (NO), and Southern (SU). Bolivia holds significant renewable energy potential. The technical capacity for solar PV reaches up to 40 TW, and wind resources could allow for up to 260 GW of onshore capacity. Additional renewable potentials include 6.09 GW for hydro dams, 0.91 GW for run-of-river hydro, 0.88 GW for geothermal, 150 TWh/year for woody biomass, and 28.02 TWh/year for wet biomass.(Jimenez Zabalaga et al., 2024) The case study its miopic, and target the year 2050. The data retrieved is grounded in a robust technical and methodological framework (Jimenez Zabalaga et al., 2024) and (Fernandez Vazquez et al., 2024) that can be updated as new data becomes available. And include all plausible technologies that may contribute to the future operational configuration of the power system.

3.1 Scenario Definition: EPI and NZE

Two scenarios were developed. The first, referred to as the Existing Policy Implementation (EPI) scenario, assumes a steady linear increase in demand based on the updated Nationally Determined Contributions (NDCs) (Ministerio de Medio Ambiente y Agua (MMAyA), 2022), which establish specific targets for the transport and lighting sectors extended to 2050. The second scenario, Net Zero Emissions (NZE), sets the objective of achieving a 100% reduction in greenhouse gas (GHG) emissions by 2050, with a gradual yearly decrease, and incorporates a broader range of technologies to explore their potential roles in a decarbonized energy system. The detailed scenario definition methodology is explained by Jimenez Zabalaga et al. (2024).

3.2 Data Harmonization

The output data from the two-step cascade framework, originally based on a multisectoral and unified-node analysis, are harmonized to serve as direct input for the UCED model. These data include hourly time resolution and spatial disaggregation into four zones (CE, OR, NO, SU), and require no additional preprocessing. The demand is distributed across zones according to sectoral shares from the 2022 CNDC report, scaled to the projected demand for 2050. Installed Generation capacity presented in Figure 3, transmission infrastructure, and storage availability are all derived from the system expansion study developed within the two-step framework. Generation capacities are provided by technology and zone, while transmission is represented through Net Transfer Capacities (NTCs) between zones, and storage includes both hydropower reservoirs (HDAM) and BESS. Hydrological inflows and availability factors for VRE are also defined as zonal hourly averages, independent of the specific geographical locations of individual generating units. Fuel costs are estimated within the same framework and are assumed as fixed projections for the year 2050, consistent across all scenarios. All detailed datasets are available in the double publication of two-step cascade modeling and bi-directional soft-linking method, presented by Jimenez Zabalaga et al. (2024) and Fernandez Vazquez et al. (2025), for reproducibility and further use.

In contrast, certain input parameters required by the UCED model are not directly provided by the long-term expansion results from the two-step cascade framework. These include the inertia constant and system inertia bounds, droop and reserve gain settings, and techno-economic parameters of individual power plants. Typical

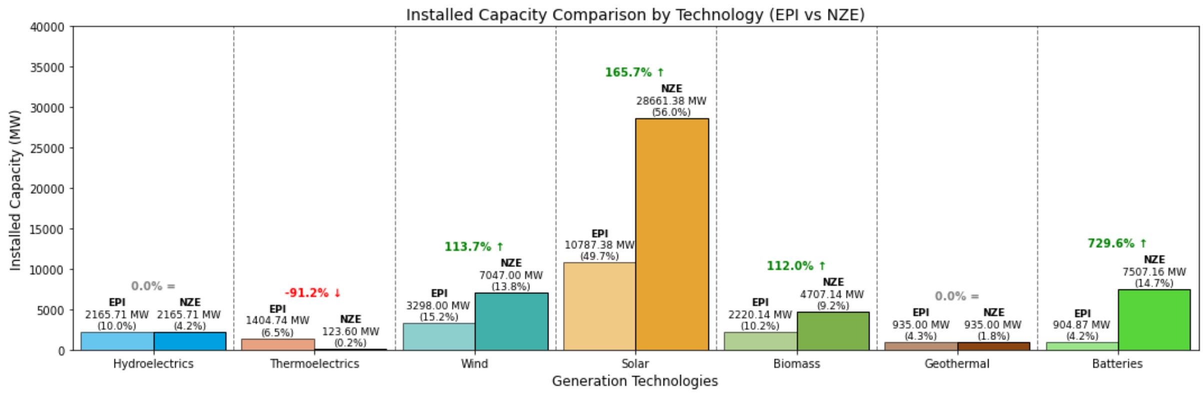

Figure 3: Installed Capacity Comparison by Technology

values are assumed for these parameters and they are presented in Table 2 and 3. For the post-fault safe operational limits, these are defined by the TSO.

Table 2: Power plant new parameters by Scenario and Technology

Scenario	Technology	Inertia Constant [s]	System Inertia Lower Bound [GWs]	System Inertia Upper Bound [GWs]	Droop [%]	Primary Gain Lower Bound [MW/Hz]	Primary Gain Upper Bound [MW/Hz]	Fast Gain Lower Bound [MW/Hz]	Fast Gain Upper Bound [MW/Hz]
EPI	HDAM	4	1	30	5	100	2650	-	-
	COMC, STUR, GTUR	5	1	30	5	100	2650	-	-
	BAT	-	-	-	2	-	-	50	900
NZE	HDAM	4	1	37	5	100	3150	-	-
	COMC, STUR, GTUR	5	1	37	5	100	3150	-	-
	BAT	-	-	-	2	-	-	200	7500

Table 3: Techno-economic data for the power plants

Technology [n.a.]	Fuel [n.a.]	Efficiency [%]	Ramping Rate [%]	StartUp Cost [EUR]	Ramping Cost [EUR]	PartLoad Min [%]	CO2 Intensity [kgco2, eq /MWh]	STO Charging Efficiency [%]
GTUR	Gas	0.32	0.06	25	0.8	0.3	0.62	-
GTUR	Oil	0.37	0.06	25	0.8	0.3	0.67	-
CCOM	Gas	0.46	0.06	25	0.8	0.3	0.43	-
STUR	Bio	0.29	0.02	120	1.3	0.3	0	-
HDAM	Wat	0.9	0.06	0	0	0.3	0	0.9
PHOT	Sun	1	0.02	0	0	0	0	-
WTON	Sun	1	0.02	0	0	0	0	-

4 RESULTS AND DISCUSSION

4.1 Stability assessment

4.1.1 Results with PFR services:

Referring to the year 2022 taken as the reference year to build up the scenarios, it is observed that the (n-1) contingency hypothesis for that specific year is 194 [MW], corresponding to the Sehuencas power plant. For this contingency, the minimum required inertia is 25 [GWs]. However, in the EPI and NZE scenarios, the projected (n-1) contingencies for 2050 would be 400 [MW], corresponding to the Rositas power plant. This represents a 106% increase in the magnitude of the (n-1) contingency. Therefore, with the maximum available system inertia and primary reserve gain, the model becomes unfeasible. Table 4 presents the results of the power swing equation, where it is observed that the system becomes stable at an inertia of 50 [GWs]. However, in future power systems with high renewable energy penetration, these levels of inertia, which typically come from conventional generation units, will not be available.

Therefore, in this work, the implementation of the FFR service is proposed, which involves the injection of active power 1 second after a contingency occurs. This power injection is provided by BESS.

Table 4: Results of the power swing equation for different inertia values

Contingency	Contingency [MW]	System Inertia [GWs]	PFR Gain [MW/Hz]	Primary Reserve [MW]	Min Frequency [Hz]	Min RoCoF [Hz/s]	Frequency Nadir [Hz]	RoCoF [Hz/s]	State
1	194	25	500	194	49.2	-0.2	49.21	-0.19	Stable
2	400	25	500	400			48.31	-0.4	Unstable
3	400	30	500	400			48.57	-0.33	Unstable
4	400	40	500	400			48.91	-0.25	Unstable
5	400	50	500	400			49.2	-0.2	Stable

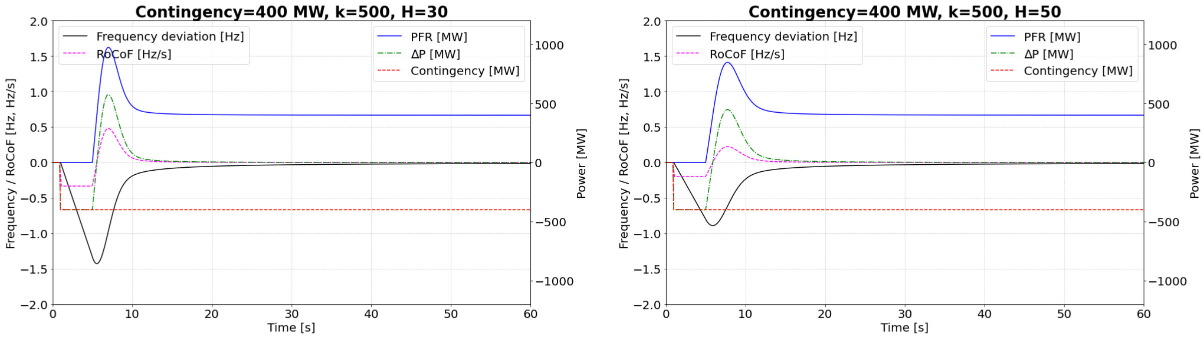

(a) Frequency and Power Excursion for Contingency 3 (b) Frequency and Power Excursion for Contingency 5

Figure 4: Comparison of Frequency and Power Excursions for Contingencies 3 and 5

4.1.2 Results with combined FFR and PFR services:

Table 5 presents the results of the power swing equation, incorporating different values of FFR. The results indicate that the minimum RoCoF threshold of 0.5 Hz/s is met, as FFR is activated one second after the contingency. This allows frequency recovery before reaching critical levels below 49.2 Hz. Various combinations of FFR gain and reserve can stabilize the system; however, all these solutions require the subsequent activation of PFR.

Table 5: Power swing equation results with the incorporation of fast frequency reserves.

Contingency	Contingency [MW]	System Inertia [GWs]	FFR Gain [MW/Hz]	Fast Frequency Reserve [MW]	PFR Gain [MW/Hz]	Primary Reserve [MW]	Min Frequency [Hz]	Min RoCoF [Hz/s]	Frequency Nadir [Hz]	RoCoF [Hz/s]	State
6	400	25	100	70	500	330	49.2	-0.5	48.85	-0.39	Unstable
7	400	25	200	120	500	280			49.11	-0.38	Unstable
8	400	25	300	155	500	245			49.23	-0.38	Stable
9	400	25	400	185	500	215			49.31	-0.40	Stable
10	400	25	500	205	500	195			49.35	-0.40	Stable

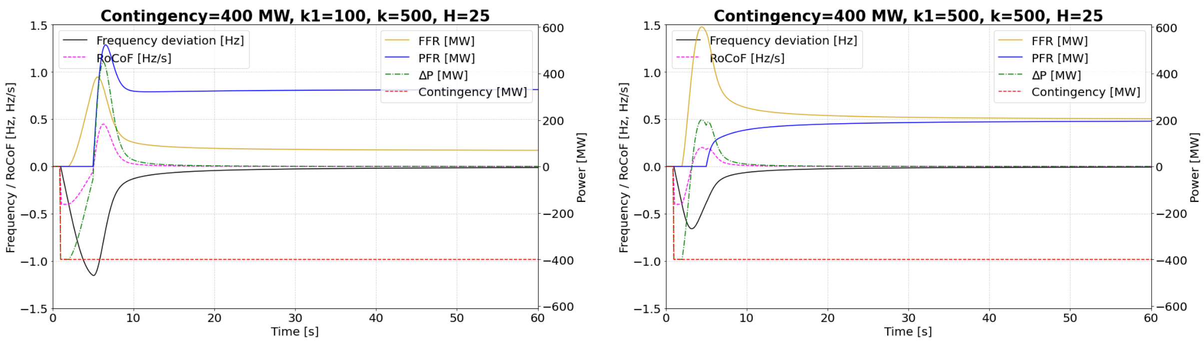

(a) Frequency and Power Excursion for Contingency 6 (b) Frequency and Power Excursion for Contingency 10

Figure 5: Comparison of Frequency and Power Excursions for Contingencies 6 and 10

4.2 Impact of frequency stability and reserve requirements

As explained in the methodology, the simulations are conducted with three different approaches. The reference approach or None Constraints (NC) serves as a benchmark and is a scenario without any stability requirements. The second approach with Static Constraints (SC) and the third approach with Dynamic Constraints (DC) incorporate stability requirements. The results, presented as averages and percentages, are summarized in Table 6, which highlights key variables.

Table 6: Table Summary of Results

Scenario	Approach	Inertia [GWs]	FFR [MW]	Average PFR [MW]	Spillage [MW]	Emissions [kgCO$_2$,eq/MWh]	Shadow Price [eur/MWh]	VRE Pentration [%]	VRE Curtailment [%]
EPI	NC	13.35	0	0	41.29	189.51	303.09	54.26	2.76
EPI	DC	19.78 (↑48.1%)	321.71 (-%)	87.31 (-%)	41.52 (↑0.6%)	203.96 (↑7.6%)	637.52 (↑110.2%)	50.76 (↓6.4%)	10.28 (↑272.5%)
EPI	SC	28.26 (↑111.7%)	495.05 (-%)	99.35 (-%)	39.92 (↓3.3%)	245.63 (↑29.6%)	803.27 (↑165.0%)	44.46 (↓18.0%)	22.63 (↑719.2%)
NZE	NC	16.27	0	0	52.73	122.07	115.09	65.42	4.12
NZE	DC	22.15 (↑36.1%)	1033.08 (-%)	102.13 (-%)	67.84 (↑28.6%)	119.51 (↓2.1%)	140.22 (↑21.8%)	63.95 (↓2.2%)	6.46 (↑56.8%)
NZE	SC	27.96 (↑71.9%)	1108.09 (-%)	116.86 (-%)	60.74 (↑15.2%)	116.56 (↓4.5%)	140.24 (↑21.8%)	61.69 (↓5.7%)	9.73 (↑136.2%)

Incorporating frequency stability constraints in UCED models significantly affects dispatch decisions, renewable integration, and system costs, highlighting the trade-off between security and economic efficiency. In the EPI scenarios, the implementation of DC approach compels the system to operate with higher levels of inertia—an increase of 48.1%—and necessitates the activation of FFR and PFR, which were absent in the NC approach. Daily average system inertia is presented in Figure 6. This increased operational demand results in a sharp rise in the marginal cost of electricity (from 303.09 to 637.52 EUR/MWh), driven by the forced dispatch of synchronous units with greater inertia or frequency response capabilities—often thermal plants—that displace renewable generation. This dynamic becomes more pronounced under SC approach, where system inertia reaches 28.26 GWs (more than double that of the baseline), and both PFR and FFR requirements grow even further. Consequently, electricity prices climb to 803.27 EUR/MWh, VRE penetration decreases significantly (a 18.0% drop), and VRE curtailment surges (a 719.2% increase). This reduced VRE penetration leads to a substantial rise in specific CO_2 emissions (245.63 $kgCO_2eq/MWh$), highlighting a critical operational trade-off in which prioritizing system stability comes at the expense of environmental performance and economic efficiency.

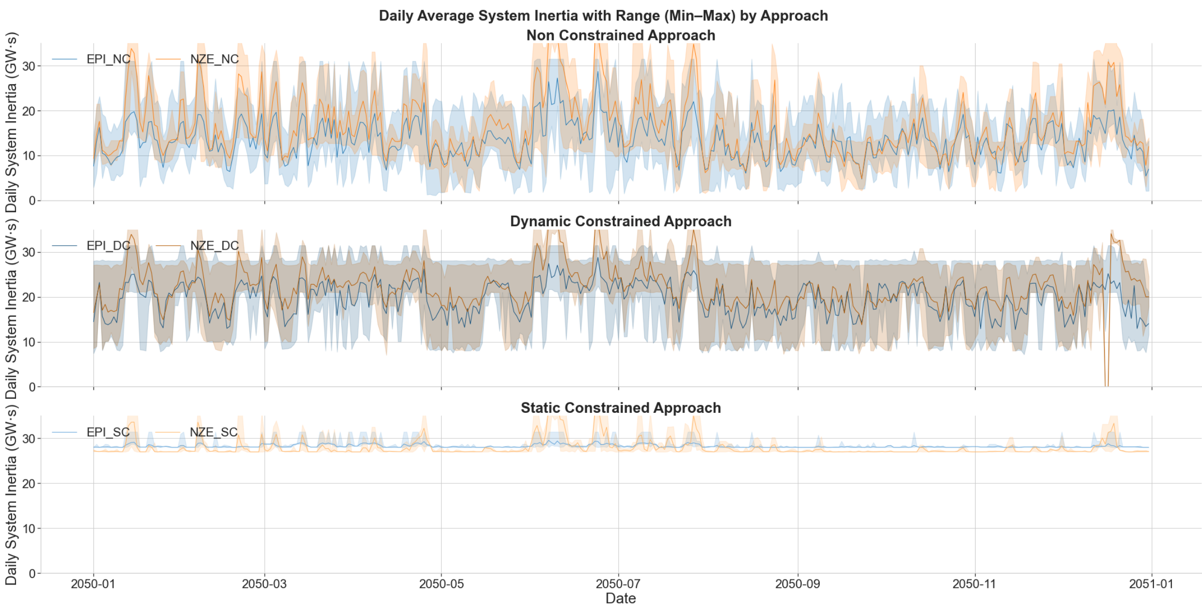

Figure 6: Comparison between Timeseries Daily Average System Inertia

In the NZE scenarios, where the generation mix is inherently more renewable-intensive, the impact of stability constraints, though less severe in relative terms, remains both operationally and economically relevant. Under DC approach, inertia rises by 36.1%, and FFR and PFR are activated, indicating that even in deeply decarbonized systems, there remains a need for flexible and responsive resources. This need is particularly evident in the case of FFR, which surges from 0 MW in the NC approach to over 1,000 MW in both DC and SC approaches. This significant increase can be attributed to multiple structural elements of the NZE system: firstly, the total annual demand nearly doubles compared to EPI (90.3 TWh vs. 47.5 TWh), which inherently raises the system's exposure to imbalances; secondly, the NZE generation mix shows a considerable expansion of VRE, with installed solar and wind capacities reaching 28.7 GW and 7.0 GW, respectively—more than double the EPI levels. The high share of non-synchronous generation results in a system with lower inertia-to-demand ratio, making it more sensitive to disturbances and increasing the critical role of FFR services. Furthermore, the NZE scenario includes 7.5 GW of installed battery capacity (compared to only 0.9 GW in EPI), which provides a technologically feasible and economically viable option for FFR provision. Interestingly, the activation of these FFR services does not lead to a substantial rise in marginal costs, which remain stable around 140 EUR/MWh, suggesting that the system's inherent flexibility—especially through storage—effectively absorbs the additional frequency stability burden without significant economic penalty.

Regarding PFR, the results suggest that this reserve is persistently deployed near its system-wide maximum capability across both DC and SC cases. The structural decarbonization and the high reliance on inverter-based resources in NZE scenarios offer a larger battery capacity available to provide FFR and PFR averaging between 300 MW and 1100 MW across the year. The marginal cost increases moderately to 140.22 EUR/MWh, with a slight decline in total generation. Despite the assumed technological flexibility of the NZE scenario, significant increases in renewable curtailment (4.57 TWh, +56%) and minor load shedding (0.02 TWh, doubling the baseline value) are observed—clear indicators of a system operating under tighter security margins. When static constraints are introduced, these trends become more pronounced: higher inertia and reserve requirements are imposed, curtailment rises to 6.89 TWh, and renewable penetration drops by 5.7%, partially undermining the primary objective of the NZE pathway. However, unlike in EPI, specific CO_2 emissions slightly decrease, which can be attributed to the structural dominance of clean technologies in the generation mix.

4.3 Dispatch Comparison between modeling frameworks and assessment of accuracy and errors

The data presented in Table 7 reveal notable divergences in dispatch outcomes between the ESOM and UCED modeling frameworks under varying operational constraints. These divergences confirm that incorporating operational constraints, as implemented in UCED, significantly alters the generation mix outcomes compared to ESOM. For hydro and geothermal technologies—both synchronous generators without explicit fuel price considerations—UCED consistently dispatches more hydro than ESOM across all approaches and scenarios. In the NZE scenario, hydro generation in UCED increases by 28.2%, 21.6%, and 22.0% under NC, DC, and SC conditions, respectively. Geothermal output, in contrast, is slightly lower in UCED, with reductions between 7.8% and 10.0%, likely due to dispatch priorities under system-level stability constraints.

Table 7: Dispatch comparison between frameworks and different approaches

Scenario	Modeling Framework	Approach	Hydro [TWh]	Thermal [TWh]	Wind [TWh]	Solar [TWh]	Biomass [TWh]	Geothermal [TWh]	Batteries [TWh]	Curtailment [TWh]
EPI	ESOM	NC	9.27	0.04	7.59	19.73	3.22	8.17	2.21	5.87
EPI	UCED	NC	11.46 (↑23.6%)	1.98 (-%)	8.37 (↑10.3%)	19.09 (↓3.2%)	1.22 (↓62.1%)	6.84 (↓16.3%)	1.64 (↓25.8%)	0.78 (↓86.7%)
EPI	UCED	DC	11.32 (↑22.1%)	2.22 (-%)	7.51 (↓1.1%)	17.63 (↓10.7%)	3.31 (↑2.8%)	6.68 (↓18.2%)	0.88 (↓60.2%)	2.88 (↓50.9%)
EPI	UCED	SC	10.91 (↑17.7%)	3.13 (-%)	6.18 (↓18.6%)	15.48 (↓21.5%)	6.73 (↑109%)	5.74 (↓29.7%)	0.57 (↓74.2%)	6.34 (↑8.0%)
NZE	ESOM	NC	9.14	0.0009	16.89	53.97	5.91	7.82	13.53	3.53
NZE	UCED	NC	11.72 (↑28.2%)	0.66 (-%)	17.16 (↑1.6%)	50.95 (↓5.6%)	6.16 (↑4.2%)	7.21 (↓7.8%)	10.25 (↓24.2%)	2.93 (↓17.0%)
NZE	UCED	DC	11.11 (↑21.6%)	0.62 (-%)	16.78 (↓0.7%)	49.39 (↓8.5%)	8.53 (↑44.4%)	7.14 (↓8.7%)	9.89 (↓26.9%)	4.57 (↑29.5%)
NZE	UCED	SC	11.15 (↑22.0%)	0.59 (-%)	16.25 (↓3.8%)	47.69 (↓11.6%)	10.57 (↑78.9%)	7.04 (↓10.0%)	10.34 (↓23.6%)	6.89 (↑95.2%)

For thermal and biomass units—also synchronous generators but with explicit fuel costs—the divergence is more pronounced. In the EPI scenario, thermal generation in UCED rises from 1.98 TWh under NC to 3.13 TWh under SC, compared to a marginal 0.04 TWh in ESOM. This increase reflects UCED's sensitivity to dynamic system constraints such as inertia and ramping, which increase the value of flexible thermal units despite higher operational costs. Biomass generation also increases substantially, especially under SC conditions in both scenarios, reaching +109% in EPI and +78.9% in NZE compared to ESOM.

Variable renewable technologies are the most affected by system security constraints. Compared to ESOM, UCED results in a consistent decrease in solar output as constraints tighten. In the NZE scenario, solar generation drops by 5.6% in NC, 8.5% in DC, and 11.6% in SC. Wind generation follows a similar trend, with a reduction of –3.8% in NZE and –18.6% in EPI under SC conditions. These results illustrate how frequency-related constraints—such as minimum inertia requirements and reserve provision—can impact the dispatch of non-synchronous, weather-dependent technologies.

Battery dispatch is also reduced across all UCED variants relative to ESOM. In the EPI scenario, battery output decreases from 2.21 TWh in ESOM to 0.57 TWh under SC (–74.2%). In NZE, the reduction ranges from –24.2%

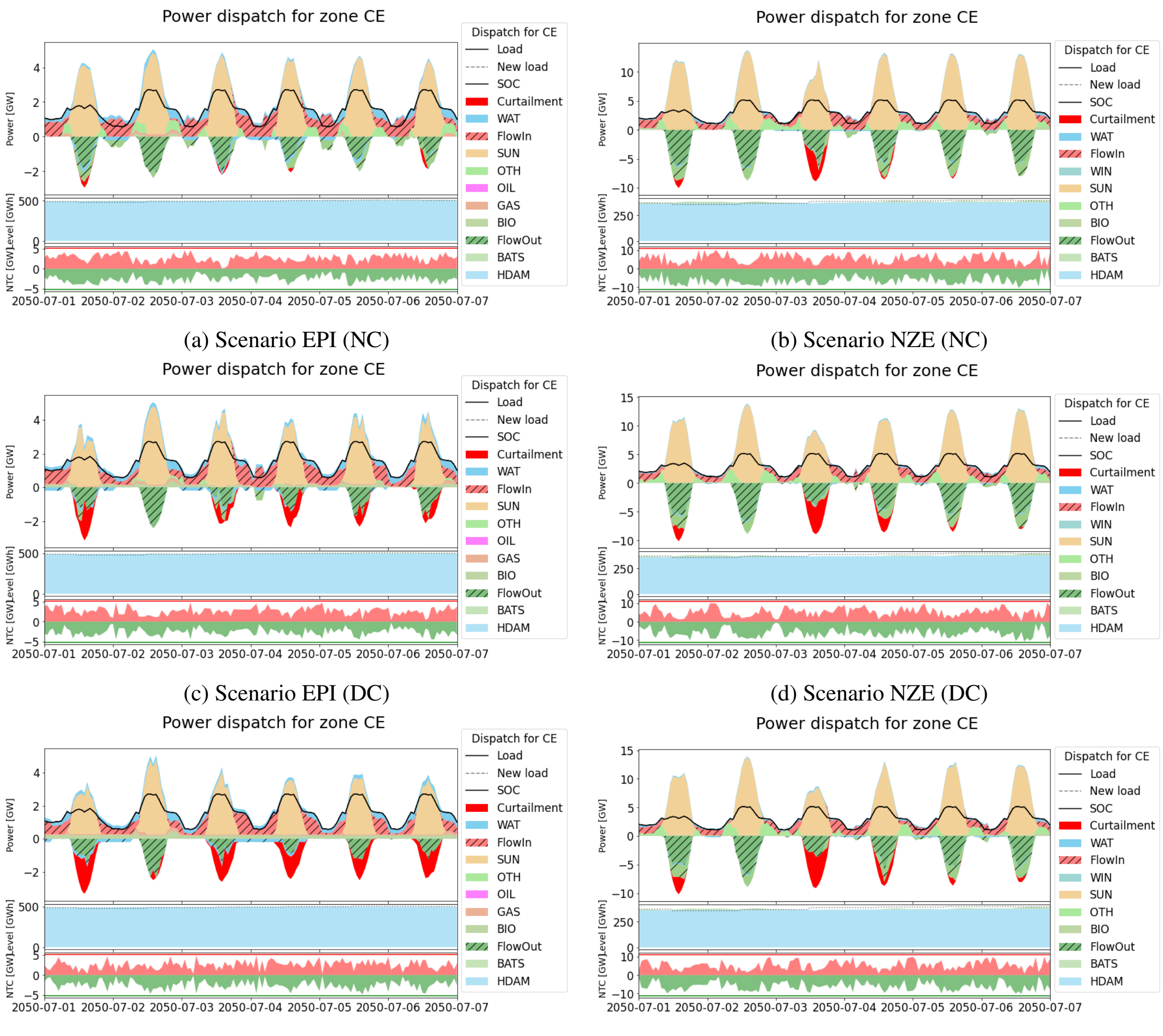

(a) Scenario EPI (NC)

(b) Scenario NZE (NC)

(c) Scenario EPI (DC)

(d) Scenario NZE (DC)

(e) Scenario EPI (SC)

(f) Scenario NZE (SC)

Figure 7: Energy Balance for different scenarios of simulation. Zone CE, from 2050-07-01 to 2050-07-07

to –26.9%. This reduction indicates that under stricter system constraints, storage operation may be deprioritized due to limited contribution to system inertia or frequency support, depending on modeling assumptions.

Curtailment shows the opposite trend, increasing substantially as operational constraints become more binding. In the NZE SC case, curtailment nearly doubles relative to ESOM (+95.2%), while in EPI SC it increases by 8.0%. This indicates reduced system flexibility to integrate variable generation under strict stability requirements.

In summary, the data expose the share divergences between ESOM and UCED, driven by the presence or absence of operational constraints in the modeling framework. These results highlight the importance of including dynamic and frequency-related constraints in capacity expansion and dispatch modeling to produce realistic and implementable generation pathways.

5 CONCLUSIONS

This study presents a modelling framework that integrates ESOM with UCED models to assess the technical feasibility of expansion plans under operational and stability constraints. By bridging the methodological gap between long-term planning and short-term operation, this approach provides a more holistic evaluation of energy transition pathways. From a modelling perspective, the integration of ESOM-based long-term planning with UCED-based operational detail reveals critical trade-offs between economic efficiency and operational reliability. While ESOM-derived scenarios are effective in outlining decarbonization trajectories, they tend to produce overly optimistic shares of VRE, primarily influenced by policy-driven emission targets. These pathways often overlook

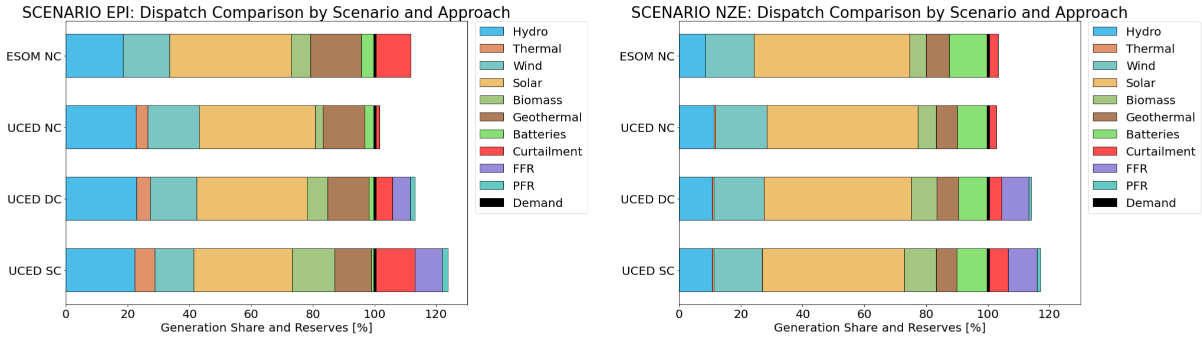

(a) Scenario EPI (b) Scenario NZE

Figure 8: Dispatch results comparison by scenario and approach

essential operational constraints such as system inertia and reserve requirements, underestimating the need for flexible, dispatchable resources and frequency support services. UCED models, in contrast, incorporate technical constraints that capture frequency stability and reserve dynamics, uncovering system-level impacts not visible in long-term planning models alone. When these constraints are considered, VRE deployment is moderated, curtailment increases, and reliance on thermal generation grows—highlighting the importance of setting realistic deployment thresholds to avoid excessive overcapacity and unanticipated system costs. These findings underscore the necessity of integrating both planning and operational layers to ensure technically viable and economically sound energy transitions. The broader implications extend to global decarbonization efforts, particularly in developing countries where power systems often operate with limited flexibility and infrastructure. As these regions pursue net-zero objectives, ensuring frequency stability becomes a limiting factor. Grid-forming inverters and BESS with FFR capabilities emerge as key enablers of secure VRE integration. Prioritizing these technologies, along with the proper valuation of the services they provide, is essential. In this regard, incorporating shadow prices for dynamic services like inertia and FFR within UCED frameworks can inform system design and resource allocation based on their operational value. Future work could build upon this study by addressing current limitations, such as assuming perfect foresight and excluding reserve co-optimization, to better capture system dynamics and the role of frequency-related services.

NOMENCLATURE

Abbreviations

SDGs	Sustainable Development Goals	RoCoF	Rate of Change of Frequency
GHG	Greenhouse gas	NDCs	Nationally Determined Contributions
MMAyA	Ministerio de Medio Ambiente y Agua	TSO	Transmission System Operator
ESOM	Energy System Optimization Model	NZE	Net Zero Emissions
UCED	Unit Commitment and Economic Dispatch	EPI	Existing Policy Implementation
GEP	Generation Expansion Planning	CE	Central Zone
VRE	Variable Renewable Energy	OR	Oriental Zone
BESS	Battery Energy Storage Systems	NO	North Zone
SIR	System Inertia Response	SU	South Zone
PFR	Primary Frequency Reserve	NC	None Stability Constraints approach
FFR	Fast Frequency Reserve	SC	Static Stability Constraint approach
PFSOL	Post-fault Safe Operational Limits	DC	Dynamic Stability Constraint approach

Latin Symbols

$RoCoF$	Rate of Change of Frequency, Hz/s or pu	$\Delta fssmax$	Frequency at the steady state, Hz
$fnadir$	Frequency nadir, Hz	Δf_{COI}	Frequency of the Center Of Inertia, Hz

Sets

i	Time step in the optimization horizon	cu	Conventional units only
t	Time step in the power-swing solution	ba	Batteries only

REFERENCES

The Dispa-SET model — Documentation. (n.d.). Retrieved April 4, 2025, from https://www.dispaset.eu/en/latest/index.html

Fernandez Vazquez, C. A. A., Jimenez Zabalaga, P. A., Balderrama, S., Cardozo, E., Jeanmart, H., & Quoilin, S. (2025). A bi-directional soft-linking method for a whole energy system model and a power system optimization model. application and analysis for the bolivian case. *Manuscript submitted for publication*.

Fernandez Vazquez, C. A. A., Jimenez Zabalaga, P. A., Balderrama Subieta, S. L., & Quoilin, S. (2024). A two-step cascade modelling between EnergyScope Pathway-BO and PyPSA-BO for energy transition planning. Part B: Geo-spatial characterization and effects. Retrieved April 1, 2025, from https://orbi.uliege.be/handle/2268/320636

Hamdi, M., El Salmawy, H. A., & Ragab, R. (2024). Incorporating operational constraints into long-term energy planning: The case of the Egyptian power system under high share of renewables. *Energy*, *300*, 131619. https://doi.org/10.1016/j.energy.2024.131619

Helgesen, P. I., & Tomasgard, A. (2018). From linking to integration of energy system models and computational general equilibrium models – Effects on equilibria and convergence. *Energy*, *159*, 1218–1233. https://doi.org/10.1016/j.energy.2018.06.146

Helistö, N., Kiviluoma, J., Holttinen, H., Lara, J. D., & Hodge, B.-M. (2019). Including operational aspects in the planning of power systems with large amounts of variable generation: A review of modeling approaches [_eprint: https://onlinelibrary.wiley.com/doi/pdf/10.1002/wene.341]. *WIREs Energy and Environment*, *8*(5), e341. https://doi.org/10.1002/wene.341

Henke, H., Dekker, M., Lombardi, F., Pietzcker, R., Fragkos, P., Zakeri, B., Rodrigues, R., Sitarz, J., Emmerling, J., Fattahi, A., Dalla Longa, F., Tatarewicz, I., Fotiou, T., Lewarski, M., Huppmann, D., Kavvadias, K., van der Zwaan, B., & Usher, W. (2024). Comparing energy system optimization models and integrated assessment models: Relevance for energy policy advice. *Open Research Europe*, *3*, 69. https://doi.org/10.12688/openreseurope.15590.2

Jimenez Zabalaga, P. A., Fernandez Vazquez, C. A. A., Limpens, G., Cardozo, E., Quoilin, S., & Jeanmart, H. (2024). A two-step cascade modelling between energyscope pathway-bo and pypsa-bo for energy transition planning. part a: Impacts of demand scenarios. *A two-step cascade modelling between EnergyScope Pathway-BO and PyPSA-BO for energy transition planning. Part A: Impacts of demand scenarios*.

Koltsaklis, N. E., Kopanos, G. M., & Georgiadis, M. C. (2017). An Optimization Framework for Power Systems Planning Considering Unit Commitment Constraints. In G. M. Kopanos, P. Liu, & M. C. Georgiadis (Eds.), *Advances in Energy Systems Engineering* (pp. 433–474). Springer International Publishing. https://doi.org/10.1007/978-3-319-42803-1_15

Navia, M., Pavičević, M., Balderrama, S., & Quoilin, S. (2023). Stability and reserve constraints in optimal dispatch models for poorly interconnected countries of the global south. *36th International Conference of Efficiency, Cost, Optimization, Simulation and Environmental Impact of Energy Systems*.

Palmintier, B., & Webster, M. (2011). Impact of unit commitment constraints on generation expansion planning with renewables [ISSN: 1944-9925]. *2011 IEEE Power and Energy Society General Meeting*, 1–7. https://doi.org/10.1109/PES.2011.6038963

Pavičević, M. (2023). Capturing the complexity of integrated energy systems through model linking - KU Leuven. Retrieved April 1, 2025, from https://kuleuven.limo.libis.be/discovery/fulldisplay/lirias4089345/32KUL_KUL:Lirias

Pavičević, M., Thiran, P., Limpens, G., Contino, F., Jeanmart, H., & Quoilin, S. (2022). Bi-directional soft-linking between a whole energy system model and a power systems model. *2022 IEEE PES/IAS PowerAfrica*, 1–5. https://doi.org/10.1109/PowerAfrica53997.2022.9905392

ACKNOWLEDGEMENT

The authors gratefully acknowledge the financial support and resources provided by the ARES-CDD and ARES PRDBOL2022 programmes, which were instrumental in the successful completion of this work.